Feasibility of hydrological application of thermal inertia from remote sensing

Valerio Tramutoli*, Pierluigi Claps*, Mauro Marella*, Nicola Pergola** and Canio Sileo***

(*) Dept. di Ingegneria e Fisica dell'Ambiente, Università della Basilicata, Potenza – Italy.

(**) Inst. Di Metedologie Avanzate per l'Analisi Ambientale – CNR – Tito (Pz) – Italy.

(***) Dept. di Ingegneria Civile, Università degli studi di Roma "Tor Vergata", Roma – Italy.

Abstract. In the context of techniques and methods for evaluation of soil water content from remote sensing, AVHRR data are considered to evaluate the possibility of using the day/night temperature difference as an indicator of the soil/canopy water content at the short time-scale.

The use of AVHRR (Advanced Very High Resolution Radiometer on board NOAA satellites) data has been proposed for indirect measures of the soil and canopy humidity to reduce, and to some extent overcome, problems related to the application of active/passive microwave data; these essentially concern the limited availability of active microwave data in terms of temporal repetition of the measure or the coarse spatial-resolution of passive sensors.

The indirect approach derives soil water content by soil-atmosphere energy balance and has the advantage of providing detailed coverage of the processes in terms of the time scale and sufficient spatial detail for the hydrological applications (1 km^2 for the AVHRR pixel Nadir view).
In this paper, surface temperature differences are used in order to evaluate the usefulness of introducing a thermal index in assessing the space-time variability of soil water content (surrogated by an Antecedent Precipitation Index - API) for purposes of initialization of flood forecasting models as well as for water balance model calibration.

For the quantitative part of this analysis we have analyzed the correlation between the day/night temperature difference, as determined by AVHRR sounding, with precipitation data from ground stations. The correlation has been evaluated over a two-year observation period on 10 precipitation stations characterized by different elevations and soil use in the surrounding areas. In this analysis the relevance and robustness of the relation between thermal inertia and API is tested and interesting implications emerge with respect to the application of this technique to infer the space/time variability of the soil water content over large areas.

Correspondence to: Dr. V. Tramutoli, Università degli Studi della Basilicata – DIFA – Contrada Macchia Romana – 85100 Potenza, ITALY
Tel: +39 0971 427209
Fax: +39 0971 427222
e-mail: tramutoli@unibas.it

1. Introduction: Methods for indirect evaluation of soil moisture

Information on the time and space evolution of soil water availability is of particular interest for hydrological applications, as related to water budget or flood frequency analysis. For scales of interest in river basin hydrology (from tens to hundreds of square kilometers), information from satellite platforms, with adequate spatial and temporal resolutions, can provide an useful support to investigate space/time variability of some hydrological parameters. In the meantime, hydrological applications of the Remote Sensing are substantially dominated by techniques and methods for evaluation of the soil water content. Most efforts are concentrated on exploiting the potential of the passive/active microwaves methods (*e.g. Engman and Chauhan*, 1995; *Schmugge*, 1998). These methods are based on sensors which are generally not suitable for an operational use, mainly because of the limited spatial resolution of passive microwaves detectors, and of the low temporal frequency and high costs of the active microwaves data. For this reason, other 'indirect' techniques for soil water evaluation based on radiometric measures in the optical range are being actively considered, mainly as part of soil-water-atmosphere models, which benefit from remote measurements of the thermal properties of the soil top layers.

A number of approaches have been proposed for indirect evaluation of soil moisture through radiometric data. A practical classification can distinguish: a) use of reflectance measurements on bare soil based on the LANDSAT-TM data (*Musick and Pelletier*, 1986); b) use of surface temperature, evaluated in the thermal infrared region (*e.g. Price*, 1980), possibly integrated by Normalized Difference Vegetation Index (NDVI) (*Carlson et al.*, 1995).

In the first approach, the limits of application are related to the low temporal frequency of the Thematic Mapper measures, that prevent from evaluating day/night soil temperature differences. The second class of methods are mainly built upon AVHRR data and present the greatest potential according to operational hydrological objectives, even because AVHRR data represent an invaluable heritage of historical information, which is essential for analysis related to long-term processes and to assessment of stationary characteristics of large areas.

The starting point of the present analysis coincides

with the 'ending' point in the *Price* (*1985*) paper, related to the use of thermal inertia for discrimination of geologic materials. Along with the significance of the topographic relief, soil moisture was in fact the main factor affecting the thermal inertia information for geological classification. This side effect is so significant to lead Price suggesting to give up with the use of thermal inertia for the main purpose of the HCMM NASA mission (*NASA*, 1978). Problems and caveats referred to the use of the remotely-sensed thermal inertia were highlighted by *Carlson* (*1986*), who pictured the useful properties of the physical parameter as well.

One of the key points we consider in the analysis of the existing and proposed models is the quantity and quality of ground data actually available for the application of methodologies. Application of Remote Sensing techniques on a regional scale has to face a limited availability of data on factors, such as air wetness, wind velocity, soil temperature, often required for the ultimate evaluation of soil moisture. Our specific interest here is related to the re-evaluation of the role of thermal inertia as an index of soil moisture. This parameter is to be viewed as an additional information to be associated to NDVI, for instance, in the context of a long-term and wide-area evaluation of the variability of soil/canopy moisture content to be used in hydrological applications.

2. The measure of Thermal Inertia from satellite

Thermal Inertia (TI) is an intrinsic property of every material, function of its conductibility (K), density (*r*) and specific heat capacity (c), according to the following relation:

$$\mathrm{TI} = \sqrt{r\mathrm{Kc}} \qquad (1$$

It represents the measure of the material resistance to the temperature changes imposed by the outside, meaning that, for a given incoming heat flux, the variation of soil temperature is inversely proportional to its thermal inertia, which is in turn influenced from soil water because of its high specific heat. Therefore it is possible to try to estimate soil water content measuring the surface temperature diurnal cycle. Water bodies, having a TI higher than the dry and wet soils, show the lowest fluctuation of temperature in daytime.

Remote sensing techniques do not allow of directly measuring the actual thermal inertia. In the specific literature there are models that, starting from remotely sensed data, are able to evaluate the real parameter but they typically need ancillary ground data, which could be not always available (*Cracknell and Xue*, 1996). A simple model is that of *Watson (1971)*, based on the assumption that the sun produces a periodic heating of the terrestrial surface and the losses of heat from the ground are entirely caused by radiative transfers. If *S* is the solar energy incident on a surface of albedo *A*, it results:

$$\mathrm{S} = \mathrm{A}\cdot\mathrm{S} + (1-\mathrm{A})\cdot\mathrm{S} \qquad (2$$

The quantity of heat absorbed by the surface, [(1-A)·S], determines an increase of the surface temperature and the amount of such increase (ΔT), depends on thermal inertia. Introducing ATI (Apparent Thermal Inertia) (*NASA*, 1978 and *Price*, 1980) as an approximate thermal inertia value and considering an area with uniform solar energy, we obtain the following relationship:

$$\mathrm{ATI} = \frac{1-\mathrm{A}}{\Delta\mathrm{T}} \qquad (3$$

where ΔT can be assumed as the difference between the maximum (T_{max}) and the minimum (T_{min}) value that the surface temperature assumes during the diurnal cycle. As such, ATI has dimension of K^{-1}.

Because of its characteristics the AVHRR is a sensor widely used to study thermal inertia from space. NOAA platforms have helio-synchronous polar orbits at low eccentricity and an average distance from earth of about 800 km. The global coverage is obtained through 14.1 orbits per day, with partial overlapping. The launching schedule makes sure that at least two sensors are in orbit at the same time, in order to offer a minimum of four daily passages over the same site of observation. From AVHRR data it is possible to get ATI estimations (*Xue and Cracknell*, 1995) computing the surface albedo from the reflectances measured in the channel 1 (0.58-0.68 μm) and channel 2 (0.7-1.1 μm) through the general formula $A = a_1R1 + a_2R2$. The coefficients a_i generally depend on the geographic latitudes of the investigated zones. The surface temperature variation is estimated by considering the difference of brightness temperatures (BT) measured in the thermal channels (around 11 μm and/or 12 μm) in two consecutive orbits, chosen in order to emphasize the diurnal thermal range ($DT = BT_{day} - BT_{night}$).

3. Methodology

The methodology of analysis is made up of the following steps: *Pre-processing:* The acquired data are calibrated (according to standard techniques as those described in *Lauritson et al.*, 1979, *Rao and Chen*, 1996), navigated, with an accuracy of the pixel order (*Pergola and Tramutoli*, 2000) and co-located all in the same geographical projection grid.

Image selection: the first criterion of selection is the time; they are chosen only the images of the same day, daytime and night-time passes, next to midnight and noon, when presumably there are the extreme (minimum and maximum) surface temperature values. The orbital characteristics of the particular selected platform (NOAA-14) allow diurnal passages in the temporal interval 12.00-14.00 PM GMT and nocturnal ones considered between 00.00 and 02.00 AM GMT. To minimize effects due to different satellite view zenith angles all the images have been rejected where the zone of interest was strongly off-nadir.

Figure 1*: Left: ATI spatial map at the 1.1 km grid resolution; black colors indicate NODATA. Right: Cumulative frequency of ATI values in Normal probability paper.*

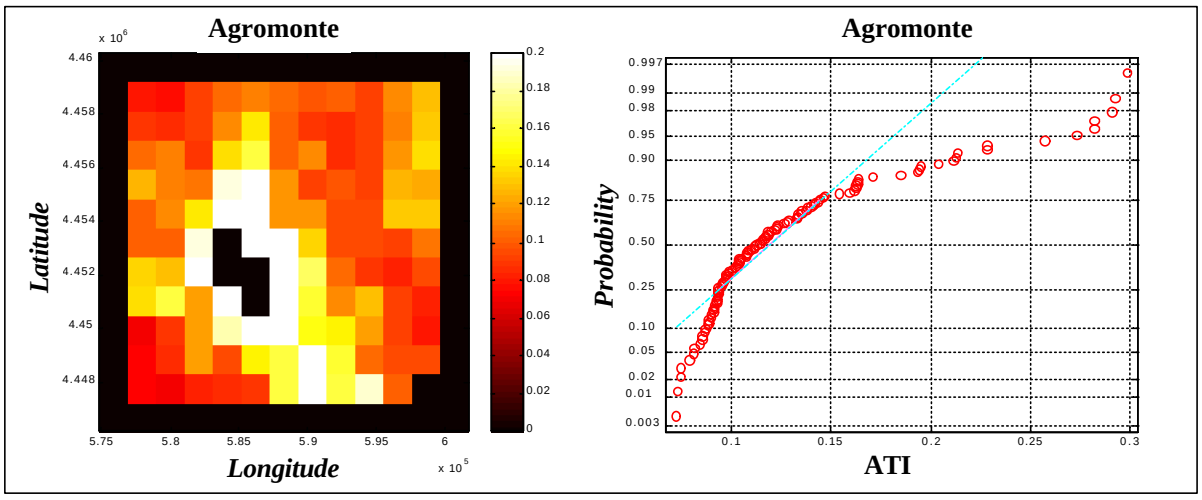

Cloud-detection: The perturbing effect due to the meteorological clouds presence in the sensor field of view has also got to be taken into consideration. In fact the measures of ATI index are possible in clear atmosphere conditions only. Therefore it is necessary either to operate clouds detection, or to identify, on the scene, the cloudy pixels in order to discard them and to get an ATI measure as reliable as possible. Widely used cloud detection algorithms (e.g. *Saunders*, 1986 and *Derrien et al*., 1993) are all defined according to a criterion of redundancy, for which it is applied more than one test to every pixel and it is identified as "clouds-free" only if all the considered tests give a negative result. The selected thresholds generally vary according to different geographical areas, to the seasonal period and to the time of image acquisition. In this particular case the identification of cloud-free pixels has been carried out by a simple cloud detection scheme, based on a single channel threshold algorithm. It's quite a "rough" scheme, chosen in order to reduce computation time, as requested by an operational approach. The test has been used on thermal infrared channel 4 for night-time passes, whereas it has been applied for both visible (channel 1) and thermal (channel 4) bands in the case of daytime orbits.

ATI map production: Finally, the ATI spatial maps are derived for the whole series of selected images, eliminating "spurious" pixels for which day-night difference of the brightness temperatures of thermal infrared channels is negative. In order to calculate the albedo, coefficients suggested by Xue and Cracknell (*1995*), suitable for mid-latitude areas, have been used. Besides the above-mentioned screening operations, frequency distribution of ATI values sometimes exhibits "anomalous" pixels (figure 1, on the right). These "outliers" are due to the roughness of the cloud detection scheme used, which allows partially cloud-contaminated pixels to survive to the screening operation and to perturb the ATI estimates. In these cases the increased value of ATI is due to a reduced value of *DT* (which appears to the denominator of ATI expression) due to a low brightness temperature of the diurnal pixel, because of the cloudy coverage. The circumstance is confirmed by the fact that pixels with increased ATI values are along the edges of those marked as cloudy (black pixel in figure 1, on the left side) and therefore influenced by the peripheral part of the cloud body. To improve the cloudy pixel screening, it has been chosen to analyze "disaggregated" data relative to *DT* and Albedo separately. By this way, considering a pixel with anomalous value of ATI, it may be possible to try to understand if the anomaly is due to clouds presence or to an anomalous increase of thermal inertia.

Since precipitation is a point measure, only one representative ATI value must be selected for comparison with the relative moisture level. In this regard, the spatial average looks not really representative of the spatial sample, because of the presence of outliers. These high values were not removed or filtered, because the median of the spatial sample was used as a robust indicator of the areal ATI values for any given day. To support this choice one can notice from the figure 1 that higher distances between the spatial average and the median occur after the rain events.

3.1 API–ATI Comparison

In order to compare the apparent thermal inertia with an indirect measure of soil water content it has been used a very simple index which considers antecedent precipitation: the API (Antecedent Precipitation Index). This represents a soil saturation index obtained by means of a composition of previous precipitations (*WMO*, 1983). The API seems to be sufficiently representative of a state of soil humidity (*Wilke and McFarland*, 1984) and it has been calculated around stations where precipitation measurements were available. There are certainly many other methods to surrogate the actual soil water content measure in the time domain but these require the measure of several ancillary variables (atmospheric and/or related to the soil). This is why they are not really useful for large areas, where the

Figure2. *Study area: Basilicata Region (Southern Italy); the map shows the degree of uniformity of land use in the boxes under study. Red dots indicate position of rainfall stations*

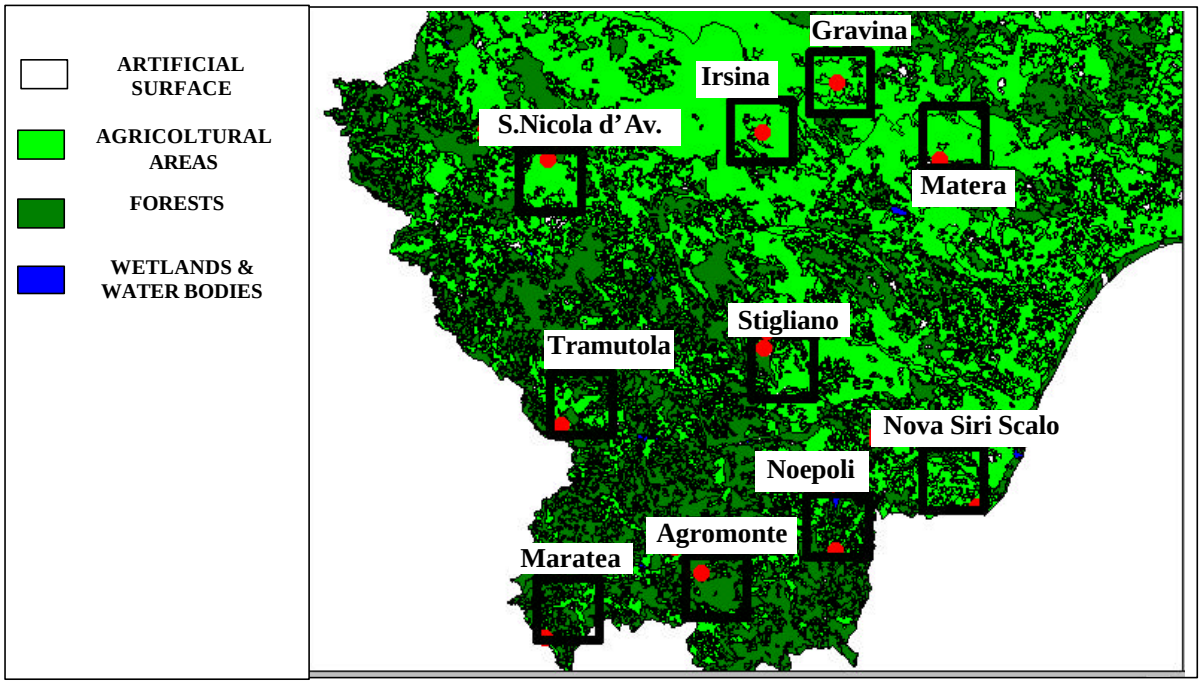

information is generally sparse. For the API it is assumed that soil moisture exponentially decreases in the dry periods according to the following relation:

$$API_i = k \cdot (API_{i-1} + P_{i-1}) \qquad (4$$

Where k is the recession coefficient and P_i is the precipitation in the *i-th* day.

The coefficient k has been calculated (*Choudhury and Blanchard*, 1983) according to:

$$k = e^{-Et/w} \qquad (5$$

where w is the equivalent soil thickness available to the evapotranspiration and Et represents the evapo-transpiration in the day t. Being k non-dimensional, API is expressed in mm. Et is computed according to the equation proposed by Hargreaves, considering the average, the maximum and the minimum daily temperatures. The lower are the values of w the lower is k and the higher is the recession rate of the API.

4. Application

The investigated area concerns ten zones located in the Basilicata region (Southern Italy) and is shown in figure 2. We have considered ten squares, about 10x10 Km in size, each containing 121 AVHRR pixels. The zones have been chosen each around a thermometric and rainfall station of the Hydrographic National Survey, making sure that there was an homogeneous land cover and small relief within the square. Comparing the thermal inertia index with the recorded meteorological data in the reference stations as well as focusing its variability considering the land cover and the average altitude, are the main purposes of present work.

The land use data come from a satellite cartography realized within the CORINE Land Cover UE Project.

Table1. *Days of the used satellite images considered.*

MONTHS	Days
May '98	21,24,26,27,28,29,30,31
June '98	3,4,16,19,20,21,22,23,24,25,27,29
July '98	3,5,6,10,13,17,19,20,21,23,24,26,27,28,29,31
August '98	1,4,12,13,15,16,17,18,21,26,27
March '99	1,9,11,12,24,27
April '99	1,2,4,5,6,13,14,19,26
May '99	6,9,10,13,25,27,28,29,30
June '99	12,14,15,21,22,23,24,26

Looking at figure 2 the zones can be divided in two main groups. The first one is characterized by coverage of a predominantly agricultural land use, dominated by crops of wheat and almost non irrigated zones. The second group contains areas with forests or dense vegetation for the greatest part.

Satellite images, all from the ASIA Database (AVHRR Historical Image Archive) of the IMAAA (Institute of Advanced Methodologies of Environmental Analysis) of the National Research Council (Tito-Potenza), have been pre-processed, selected and analyzed, according to the previously described scheme. The whole data set used is shown in table 1. For every examined day, values of ATI, Albedo and *DT*, have been calculated on every cloud-free pixels and medians have been derived for every rectangle (an example of the 3rd July 1998 is shown in table 2 only for the ATI).

Table2. *Summary of the statistical parameters derived for all the test areas for the day 03/071998.*

ATI											
Days	***Statistic quantities***	***Stations***									
		Gravina	**S. Nicola**	**Irsina**	**Matera**	**Stigliano**	**Tramutola**	**Maratea**	**Agromonte**	**Noepoli**	**NovaSiri**
03.07.98	*cloud-free pixels*	110	121	121	121	121	121	96	121	121	76
	Min	0.0344	0.0474	0.0392	0.0342	0.0393	0.0415	0.0544	0.0509	0.0428	0.0232
	Max	0.0527	0.0755	0.0568	0.0435	0.0771	0.1069	0.1001	0.1267	0.2152	0.05
	Median	0.0389	0.0551	0.0444	0.0382	0.0452	0.0497	0.0724	0.0778	0.0543	0.0359
	Mean	0.0398	0.0565	0.0447	0.0382	0.0483	0.0536	0.0721	0.0806	0.0624	0.0358
	Skew	1.4244	0.9554	0.8935	-0.1048	1.6069	2.1084	0.4922	0.3317	3.3857	0.0418
	Dev_std	0.004	0.0061	0.0037	0.0016	0.0081	0.0119	0.0102	0.0189	0.0237	0.008
	CV	0.1016	0.1075	0.0817	0.0417	0.1677	0.2221	0.1412	0.2344	0.3796	0.2245

The rainfall time history for every station has been compared to the spatial median of ATI daily values. Figure 3 shows an example derived for two stations for July 1998. At the top of the figure percentages of cloud-free pixels detected inside the station box have been reported.

It was found, that great part of the days in which ATI value increases without there has been previous rain, is characterized by a percentage less than 50% of useful (clouds-free) pixels. Then it can be supposed that the remaining data of apparent thermal inertia are influenced by badly filtered clouds and possibly produce an ATI increase without there is a real increasing of soil moisture content. To make a first evaluation of ATI index sensitivity, following an important rainy event, the most meaningful rain events have been individualized in the analyzed months, either from the point of view of the quantity of fallen rain, and/or considering their spatial distribution. We have chosen isolated events, characterized by dry periods both before and after the precipitation and for which a meaningful data set of satellite measurements was available. An example can be the one occurred on July 15th 1998.

Regarding the mentioned event, the figure 3 shows the comparison between the areal median of the ATI values and the recorded daily rains in the stations of Nova Siri and Noepoli. Immediately after the rain (17^{th} July), ATI assumes a value significantly greater than values preceding the event, either for the station of Noepoli and for the one of Nova Siri. On the other hand, on the 26^{th} the area of Nova Siri showed an increase of ATI without any corresponding rain. Examining ATI spatial maps of the considered day, it can be deduced the presence of a cloud body that involves the whole zone and has not been filtered (figure 4 on the right). Such a circumstance is confirmed by the fact that the zones of Noepoli and Stigliano, both next to Nova Siri, were completely filtered out. Furthermore, the distribution of *DT* (figure 4 on the left) in that day shows anomalous values in Nova Siri's area. All these values are lower than 3°C. The same considerations could be done also for the 6^{th} July, for the same station, as well as for the 27^{th} July, relatively to the Noepoli station.

After the rain, the median of ATI in the drying phase decreases at a different speed around Nova Siri and Noepoli. In Nova Siri (where the land cover is classified as arable land and heterogeneous agricultural areas) after only two days, ATI got back to be a comparable value to the ones of the dry period preceding the event. In Noepoli (a more vegetated area) the drying phase lasted longer.

Table 3. *Estimated equivalent soil thickness(w) and correlation coefficient (R^2)) for all test sites.*

STATION	w [mm]	R^2
Nova Siri	1,42	0,32
Irsina	3,53	0,76
Matera	5,53	0,42
Gravina	4,44	0,57
S.Nicola d'Av.	13,04	0,14
Agromonte	8,5	0,55
Tramutola	5,53	0,42
Noepoli	8,55	0,57
Maratea	1,64	0,68
Stigliano	6,43	0,52

In figure 5 the API and ATI time evolutions are shown with reference to the period of July and August 1998, for the station of Agromonte. The soil thickness *w*, for every single zone, has been calculated minimizing the difference between API and ATI for each analyzed month in 1998. Before proceeding, a standardization of ATI and corresponding API values has been accomplished. Derived *w* values, together with the corresponding correlation coefficients (R^2), are shown in table 3 for every station.

Examining the computed soil thickness values, it seems clear that they assume very small values in comparison to those which are normally found in literature. This circumstance is justified if it is considered that the index of apparent thermal inertia is a characteristic of the ground surface in its more external layers. However it is evident that *w* values on poorly vegetated areas and on areas characterized by densest vegetation assume different values.

Figure3. *ATI median values (diamonds, scale on the right) and measured precipitation (bars, scale on the left) for two selected stations (period: July 1998). Percents on top of figures indicate relative number of valid pixels in the image.*

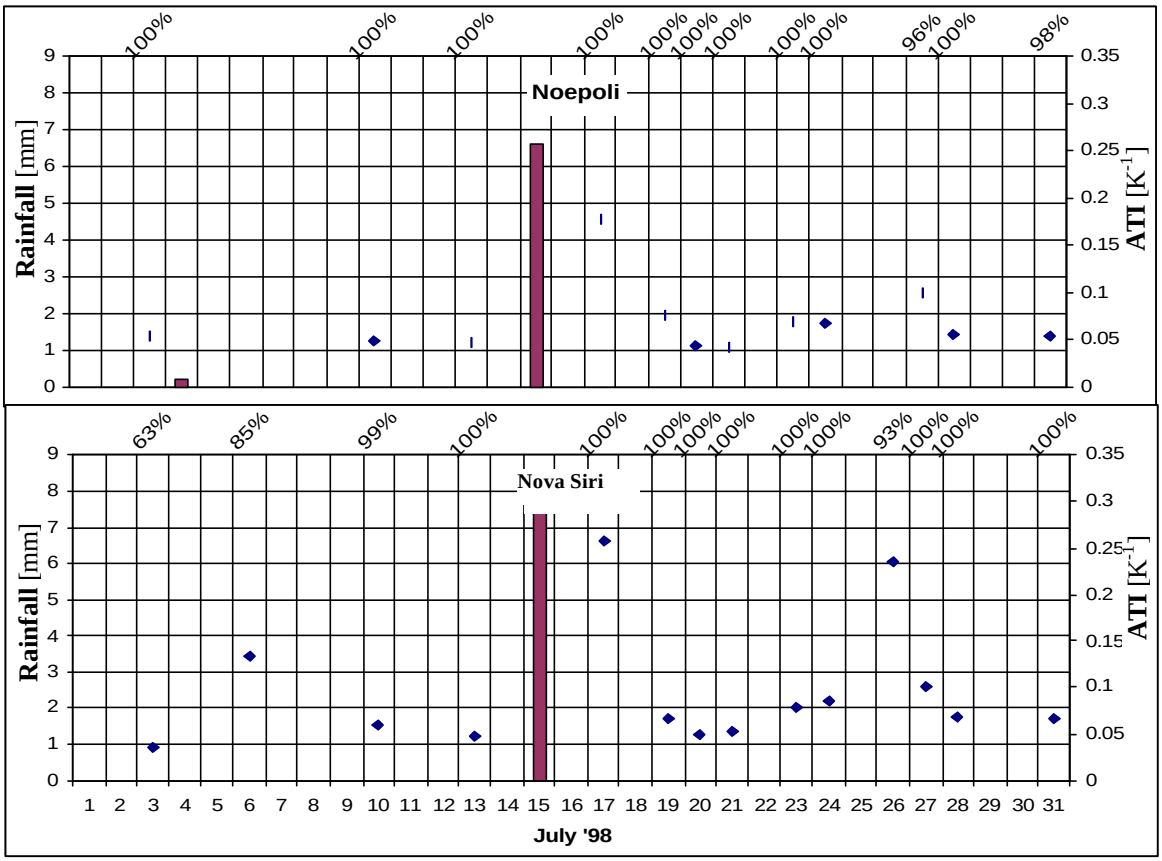

Figure 4. *Left: DTI cumulative frequency of ATI values in Nova Siri (July, 26th); Right: ATI spatial maps, derived for the ten boxes on July, 26th; note Noepoli and Stigliano areas (both next to NovaSiri station) completely masked by clouds.*

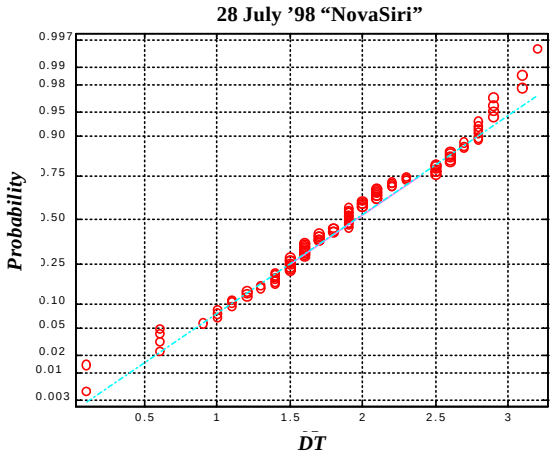

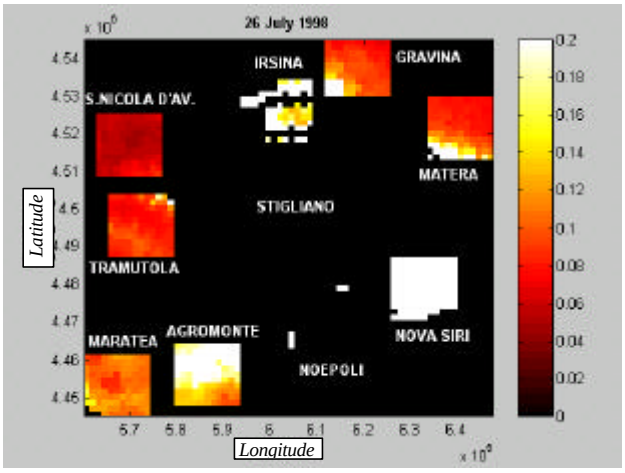

Maratea belongs to the second group because of its vegetation, but it also presents significant areas covered by bare fractured limestone formations. This explains its low value of w.

5. Conclusions

In order to asses capabilities of NOAA/AVHRR data in soil moisture estimation, a comparison between Apparent Thermal Inertia (ATI) values and precipitation has been accomplished. The analysis has been targeted towards wide–area soil moisture distribution reducing as much as possible the use of ancillary, ground-based, information. Preliminary results seem to confirm an high sensitivity of ATI to soil wetness, even through the clearing of thin clouds and cloud edges can dramatically affect the estimations

Figure 5. *ATI-API comparison for the Agromonte area (period July-August 1998). Dots represent ATI median values (scale on the right) while solid line represents API (scale on the left).*

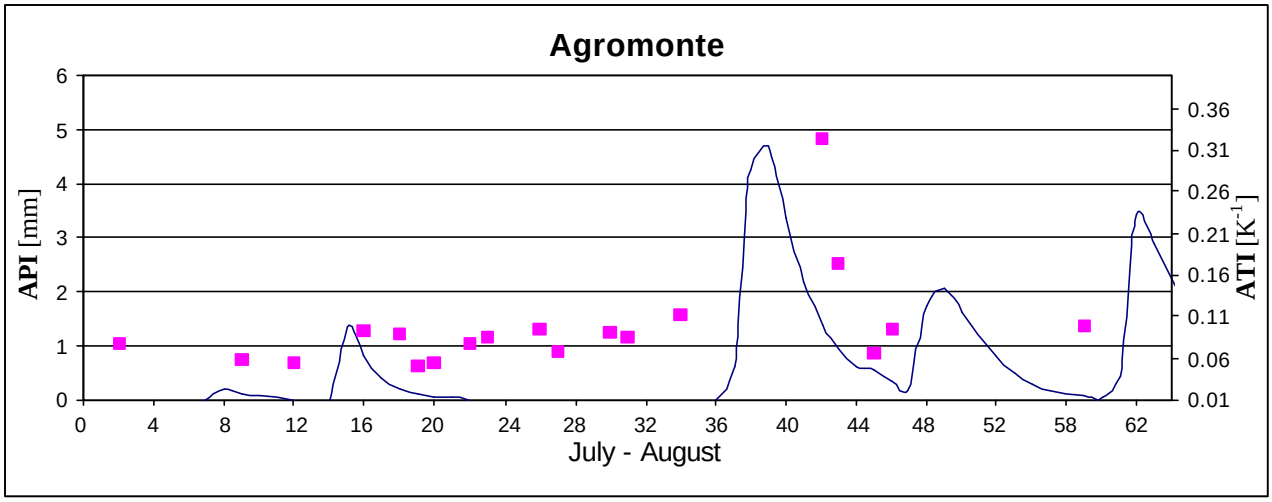

through alteration of the brightness temperature. In unperturbed conditions, however, ATI maps derived over ten different squared zones located in Southern Italy, seem to give a pretty good rendering of soil state, independently on the particular land cover. ATI sequences, obtained for two different months in two different years fit well also with the temporal evolution of the Antecedent Precipitation Index (API), for which an attempt has been made of objective calibration of the recession coefficient. A more accurate cloud-detection scheme, together with the implementation of the variability of the solar flux represent the natural improvements of this work. To face the challenge of processing cloudy images, possibilities offered by a data merging with the AMSU (Advanced Microwaves Sounding Unit) soundings, onboard new generation of NOAA platforms, could be evaluated as a future extension of such an analysis. AVHRR data can be also considered as a training tool, in the field of a possible next implementation of such techniques towards new generation satellite sensors, with improved spectral capabilities and higher temporal resolutions.

Ackowledgements

This work has been carried out within the framework of "TIMORAN" POP-FESR project, jointly funded by EU and Regione Basilicata. Funding support from MURST (Cofin 1999) and CNR-GNDCI is also acknowledged

References

Carlson, T.N., (1986) Regional – Scale Estimates of Surface Moisture Availabiity and Thermal Inertia using Remote Thermal Measurement. Remote Sensing Reviews, 1, 197-247.

Carlson, T.N., Gillier, R.R. & Schmugge, T.J. (1995) An Interpretation of Methodologies for Indirect Measurement of Soil Water Content. *Agric. and Forest Meteorol*., 77, 191-205.

Choudhury, B.J. and Blanchard, B.J. (1983) Simulating soil water recession coefficients for agricultural watersheds. *Water Resources Bulletin*, 19, 241-247.

Cracknell, A., Xue Y. (1996) Thermal inertia determination from space – a tutorial review. *International Journal of Remote Sensing*, 17(3), 431-461.

Derrien, M., Farki, B., Harang, L., Le Gleau, H., Noyalet, A., Pochic, D. and Sairouni, A., (1993) Automatic cloud detection applied to NOAA-11/AVHRR imagery. *Remote Sensing of Environment*, 46, pp. 246-267.

Engman, E.T., Chauhan, V. (1995) Status of microwave soil moisture measurements with remote sensing. *Remote Sensing of the Environment*, 51(1), 189-198.

Lauritson,L., Nelson,G.J. and Porto,F.W. (1979), Data Extraction and Calibration of TIROS-N/NOAA Radiometers. NOAA Technical Memorandum NESS 107, U.S. Department of Commerce, Washington, D.C., U.S.A.

Musick, H. B., Pelletier, R. E. (1986) Response of some thematic mapper band ratios to variation in soil water content. *Photogram. Eng. & Rem. Sens.*, 52(10) 1661-1668.

NASA (1978): Heat Capacity Mapping Mission User's Guide. NASA: Goddard Space Fluight Center, Greenbelt, Maryland

Pergola N. and V. Tramutoli (2000) SANA: Sub-pixel Automatic Navigation of AVHRR imagery. *International Journal of Remote Sensing*, 2000, 21 (12), pp. 2519-2524.

Price, J.C. (1980) The potential of remotely sensed thermal infrared data to infer surface soil moisture and evaporation. *Water Resources Research*, 16 (4),787 -795.

Price, J.C. (1985), On the analysis of thermal infrared: the limited utility of Apparent thermal inertia. *Remote Sensing of Environment*, 18, 59-73, 1985.

Rao, C.R.N. and Chen, J., (1996) Post-launch calibration of the visible and near-infrared channels of the Advanced Very High Resolution Radiometer on the NOAA-14 spacecraft. *International Journal of Remote Sensing*, 17, 2743-2747.

Saunders R.W. (1986) An automated scheme for the removal of cloud contamination from AVHRR radiances over western Europe, *International Journal of Remote Sensing*, 7,(7), pp.867-886.

Schmugge, T.J. (1998) Applications of Passive Microwave Observations of Surface Soil Moisture. *Journal of Hydrology*, 212/213, 1-4, 188-200.

Watson, K. (1971) A computer program of thermal modelling for interpretation of infrared images. *U.S. Geological Survey Report P.B.* Washington D.C.

Wilke, G.D. and McFarland, M.J. (1984). Multispectral passive microwave correlations with an antecedent precipitation index using the NIMBUS-7 SMMR, Texas A&M University Remote Sensing Center, Tech, Report RSC-141.

WMO (1983), *Guide to Meteorological Practice*, World Meteorol. Org., Publ. n. 168.

Xue, Y., Cracknell A. (1995), Advanced thermal inertia modeling, *International Journal of Remote Sensing*, 16(3), 431.